

EFW-IRFU-TN-0006
Date: 3 February 2000

Issue: 0
Rev.: 1
Page: i

Cluster EFW: Analysis of Analog and Digital Calibrations

Anders Eriksson
(aie@irfu.se)

Swedish Institute of Space Physics, Uppsala Division

Document Status Sheet			
1. Document Title: EFW Calibrations Analysis			
2. Document Reference Number: EFW-IRFU-TN-0006			
3. Issue	4. Revision	5. Date	6. Reason for Change
Draft	0	96 Feb 29	New document
Draft	1	3 Feb 2000	First draft for Cluster II

Contents

1	Introduction	1
1.1	Background	1
1.2	Scope of the document	1
1.3	Related documents	1
1.4	Definitions and acronyms	2
2	Analysis of test results	3
2.1	V1L, V2L, V3L, V4L	4
2.1.1	Similarity validation	4
2.2	V1M, V2M, V3M, V4M	6
2.3	V12M, V34M	6
2.4	V1H, V2H, V3H, V4H	6
2.5	V12H, V34H, V14H, V23H	6
2.6	V1U, V2U, V3U, V4U	6
2.7	BP34	6
2.8	SCX, SCY, SCZ	6
2.9	Reference Documents	14

This page intentionally left blank.

1 Introduction

1.1 Background

The electric field and wave experiment (EFW) of the Cluster project is designed to measure the electric field and plasma density.

The instrument will measure the wave and quasi-static electric fields in the spin plane of the four Cluster spacecraft with high time resolution. Voltage/current sweeps can also be made to measure both electron temperature and density. The three magnetic field signals from the search coil sensors are also available in the EFW experiment.

The sensors consist of 16 spherical probes, four for each of the four spacecraft. The probes can be operated in pairs to measure the voltage between probes or the voltage between a single probe and the spacecraft can be measured. The probes can also be used as low impedance probes (ampère meter) to measure the current between the plasma and the probe.

To derive the real fields in the plasma from the data telemetred to ground, we need accurate calibration of the signals and a model for the interaction between the probe-satellite system and the plasma. The latter is outside the scope of the pre-launch calibration process.

1.2 Scope of the document

The results of the analog and digital calibrations are presented in [Ref. 2] and [Ref. 6], respectively. The present document is intended to analyse and summarize the results from these reports, so as to review all input needed for the application of calibrations [Ref. 1] in one place. The emphasis is on:

- analysis of the similarity of the EFW instruments on the different Cluster satellites
- analysis of the similarity between signal paths, intended to be identical, within any single EFW instrument
- summary of the phase and amplitude responses (transfer functions) of the instruments
- derivation of poynomials describing the transfer functions, for use in data analysis

1.3 Related documents

1. The scientific user requirements on the EFW instrument are described in [Ref. 3], part 1, page 8, *Scientific capabilities*.
2. The *analog calibrations* reference document is [Ref. 2]
3. The *digital calibrations* reference document is [Ref. 6].

4. The application of the calibration products to EFW data is described in [Ref. 1].

1.4 Definitions and acronyms

See corresponding section of [Ref. 2].

2 Analysis of test results

The EFW instrument is described in [Ref. 3] and [Ref. 4]. An overview over the logical structure of EFW is given by the block diagram in Figure 1. In this diagram, the names

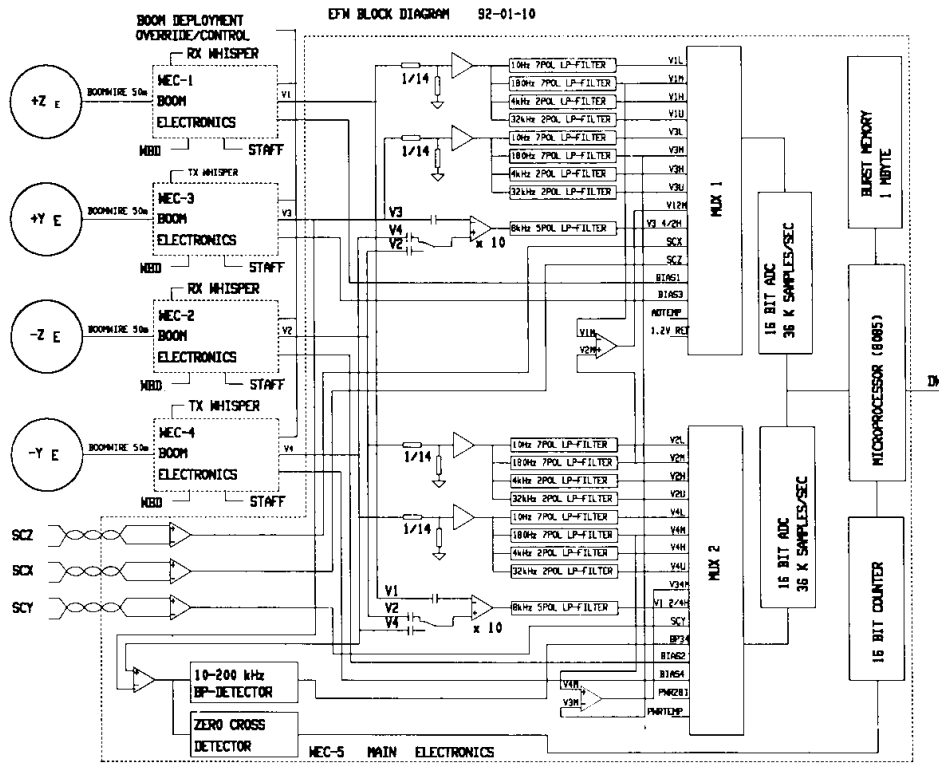


Figure 1: Block diagram of the Cluster EFW instruments.

of different signals are shown just to the left of the multiplexors (MUX1 and MUX2). These signals naturally form the following groups:

1. Lowest-frequency band, single-probe signals: V1L, V2L, V3L, V4L. These are low-pass filtered at 10 Hz and sampled at 25 sample/s.
2. Medium-frequency band signals: Low-pass filtered at 180 Hz, sampled at 450 samples/s.
 - (a) : single-probe signals: V1M, V2M, V3M, V4M
 - (b) : double-probe signals: V12M, V34M
3. Higher-frequency band signals:
 - (a) : single-probe signals: V1H, V2H, V3H, V4H. Low-pass filtered at 4 kHz, sampled at 9 ksamples/s.
 - (b) : double-probe signals: V12H, V34H, V14H, V23H. Band-pass filtered, with low-pass filter at 8 kHz, sampled at 18 ksamples/s.

4. Highest-frequency band, single-probe signals: V1U, V2U, V3U, V4U. Low-pass filtered at 32 kHz, sampled at 36 ksamples/s.
5. Signals from STAFF SC: SCX, SCY, SCZ

The digital tests of the EFW instrument are described in [Ref. 6]. In these tests, the input signal to the instruments were a sinusoidal wave of frequency f and amplitude A superposed on a DC offset B . Each of the channels V1L, V2L, ..., V1M, ..., V4U on every EFW model were tested at different values of f , A , and B (see table in Section 3.2 of [Ref. 6]). As several amplitudes and offsets were used in the tests, the test results include information on deviations from perfect linearity in the EFW instrument.

The analog tests are described in [Ref. 2]. These tests provide phase response information not present in the results from the digital tests. They also give the only information on the instrument frequency response for signals with frequency above the Nyquist frequency. Finally, we use them to compare to the results for the amplitude response function derived from the digital tests.

2.1 V1L, V2L, V3L, V4L

Note: Awaiting the completion of the EFW tests and the data therefrom, this section is included as a sample only. It is based on data from Cluster I.

2.1.1 Similarity validation

Figure 2 shows a summary of the power response curves for the V1L – V4L signals for all five EFW models as derived from these tests.

The data at left in Figure 2 is in the format of the *dtable* program, described in [Ref. 5]. By taking the maximum difference found between any two dB values for each frequency f , we form the maximum deviation $\Sigma_{\text{dB}}(f)$. Similarly, we form the standard deviation of the power response values at f , $\sigma_{\text{dB}}(f)$. From these dB values, we can calculate the corresponding amplitude deviations in per cent as

$$\Sigma_{\text{amp}} = 100 \cdot 10^{\Sigma_{\text{dB}}/20} \quad (1)$$

$$\sigma_{\text{amp}} = 100 \cdot 10^{\sigma_{\text{dB}}/20} \quad (2)$$

These quantities may be interpreted as the maximal and typical differences found when measuring a signal in two different channels, possibly also on two different spacecraft. The curves of $\Sigma_{\text{amp}}(f)$ and $\sigma_{\text{amp}}(f)$ are plotted in the right plot of Figure 2. It is seen that within the pass band of the filter (below 10 Hz), the maximum deviation is 9 % in amplitude, while a more typical value is 2 %. However, we should note that these figures include not only the differences between channels and EFW models, but also the differences in transfer function for any single channel for different input signals. If the instruments were perfectly linear, no such difference would be present, but in reality the, the amplitude of the signal as well as the DC offset may be important.

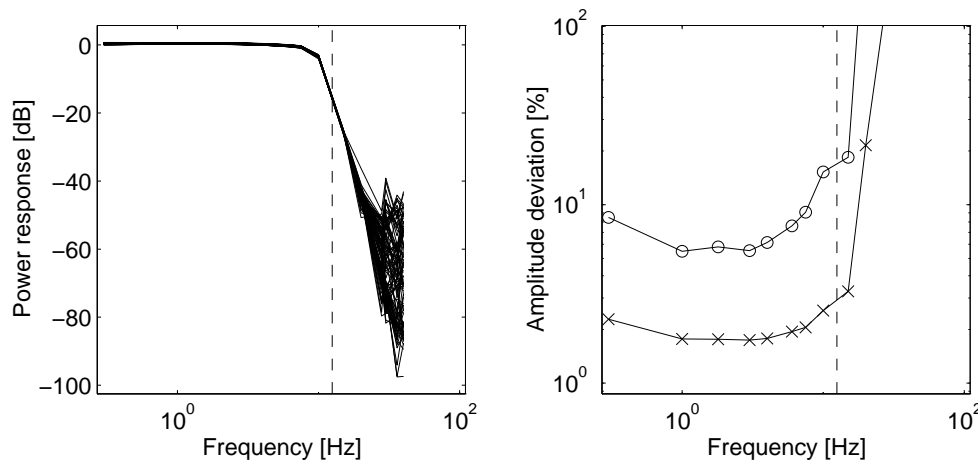


Figure 2: Summary of all digital tests of EFW V1L – V4L. Left: All power response curves. Right: Maximum (circles) and standard (crosses) amplitude deviations between channels. The Nyquist frequency is indicated by the dashed line.

Figure 3 shows separate diagrams, similar to the right plot in Figure 2, for each combination of amplitude and bias used in the test [Ref. 7, Section 3.2]. The upper left plot is the same as the right plot in Figure 2, i. e., showing results from all tests on V1L – V4L. In the other plots, each point represents data from 20 channels: V1L – V4L on each of the five EFW models F1 – F5. From these plots, it is clear that $\Sigma_{\text{amp}}(f)$ and $\sigma_{\text{amp}}(f)$ do decrease when sorting the data according to A and B . However, the maximal deviation Σ_{amp} between any two V1L – V4L channels may still be up to 10 % in the pass band, and a value σ_{amp} of 1 – 2 % is typical.

The question now arises if the spread is mainly due to peculiarities of the different models and channels, so that the uncertainties may be reduced by an individual calibration of each model or each channel. Figure 4 shows the deviations Σ_{amp} and σ_{amp} for each model. The deviations are about equal on all models, with F1 showing somewhat lower values than the other. It is also possible that the channels V1L – V4L may be different from each other but fairly identical between the models. In Figure 5, we can see that there is essentially no model-independent difference between the channels, as the deviations are about the same for all channels V1L – V4L.

Finally, we present results sorted both on models and channels. This is found in Figures 6 – 10. We can see that the spread, which now is due solely to different values of A and B in the input signal,

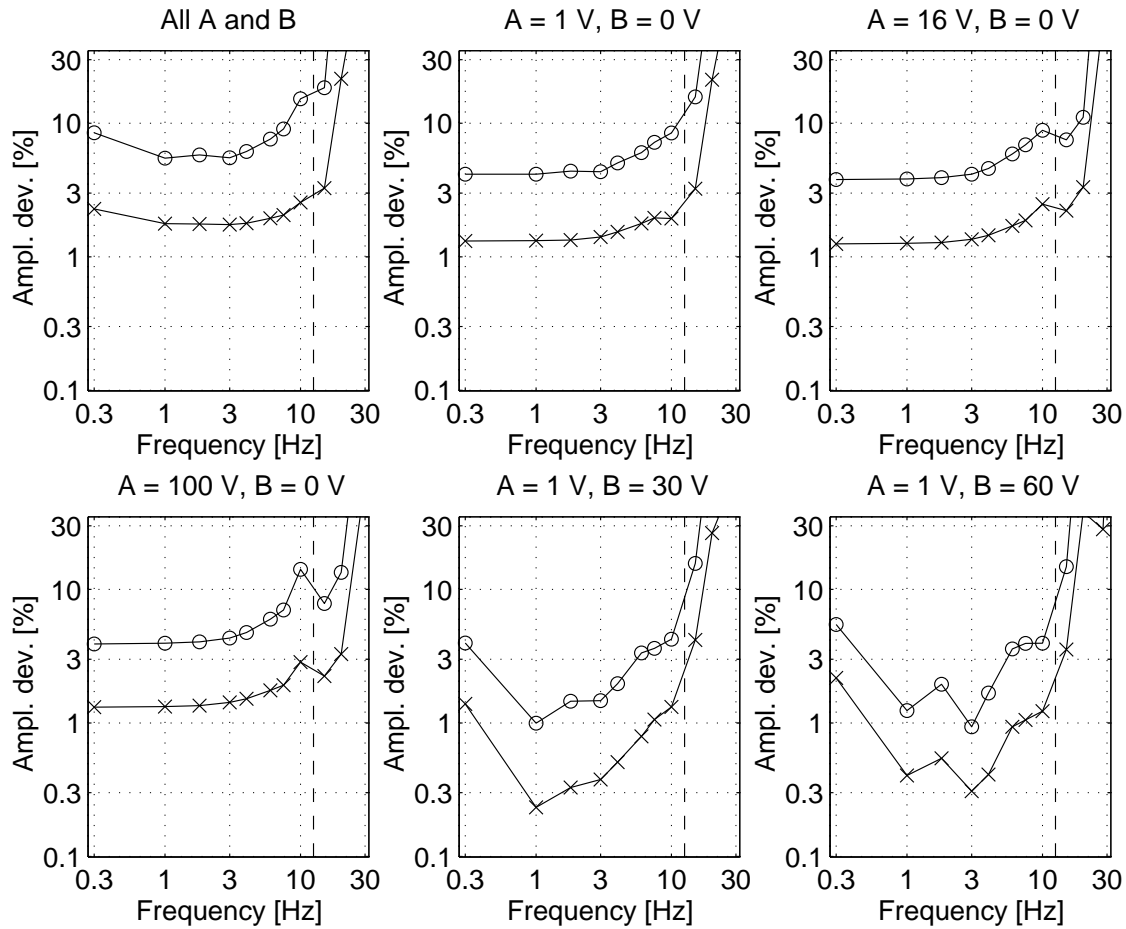


Figure 3: Maximum (circles) and standard (crosses) amplitude deviations between channels as obtained with different stimuli amplitude A and DC offset B . The Nyquist frequency is indicated by the dashed line.

2.2 V1M, V2M, V3M, V4M

2.3 V12M, V34M

2.4 V1H, V2H, V3H, V4H

2.5 V12H, V34H, V14H, V23H

2.6 V1U, V2U, V3U, V4U

2.7 BP34

2.8 SCX, SCY, SCZ

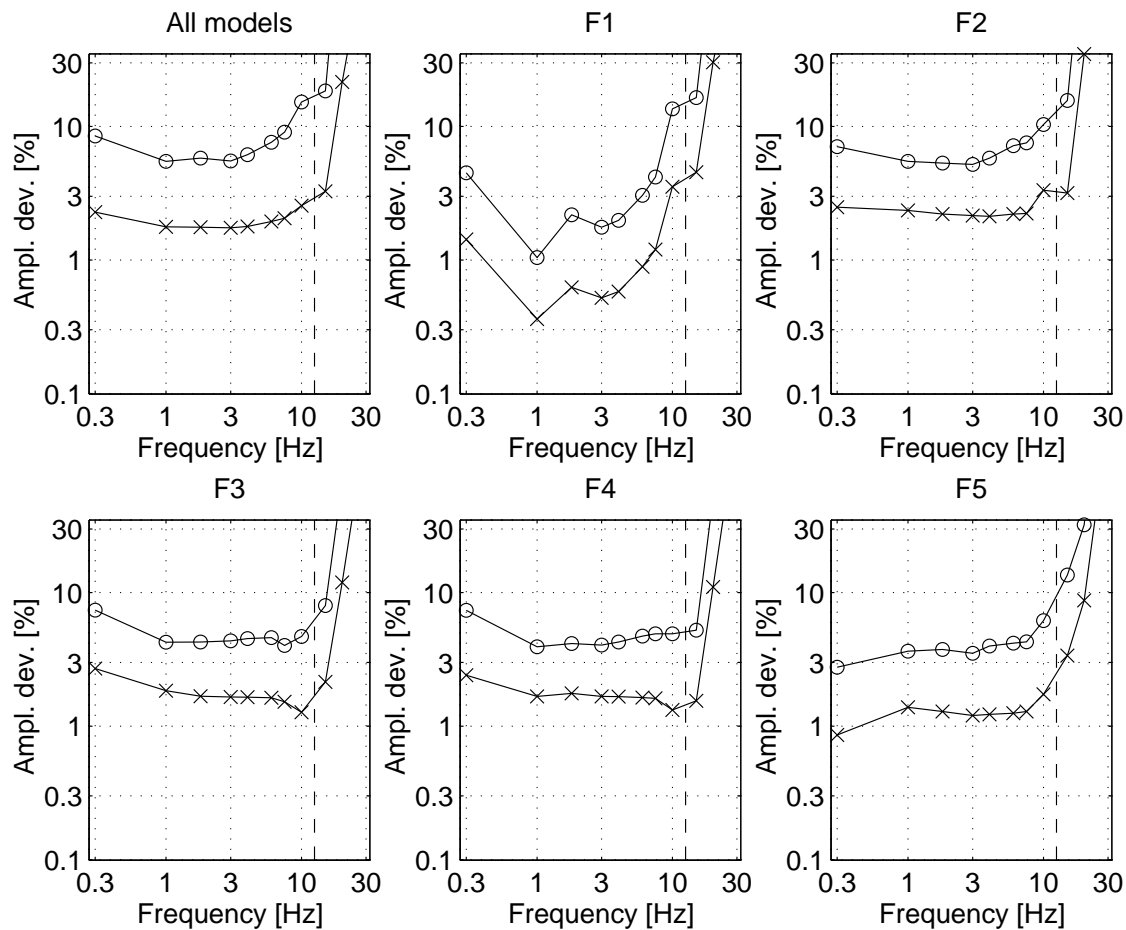


Figure 4: Maximum (circles) and standard (crosses) amplitude deviations between channels for the different EFW models. Nyquist frequency indicated by the dashed line.

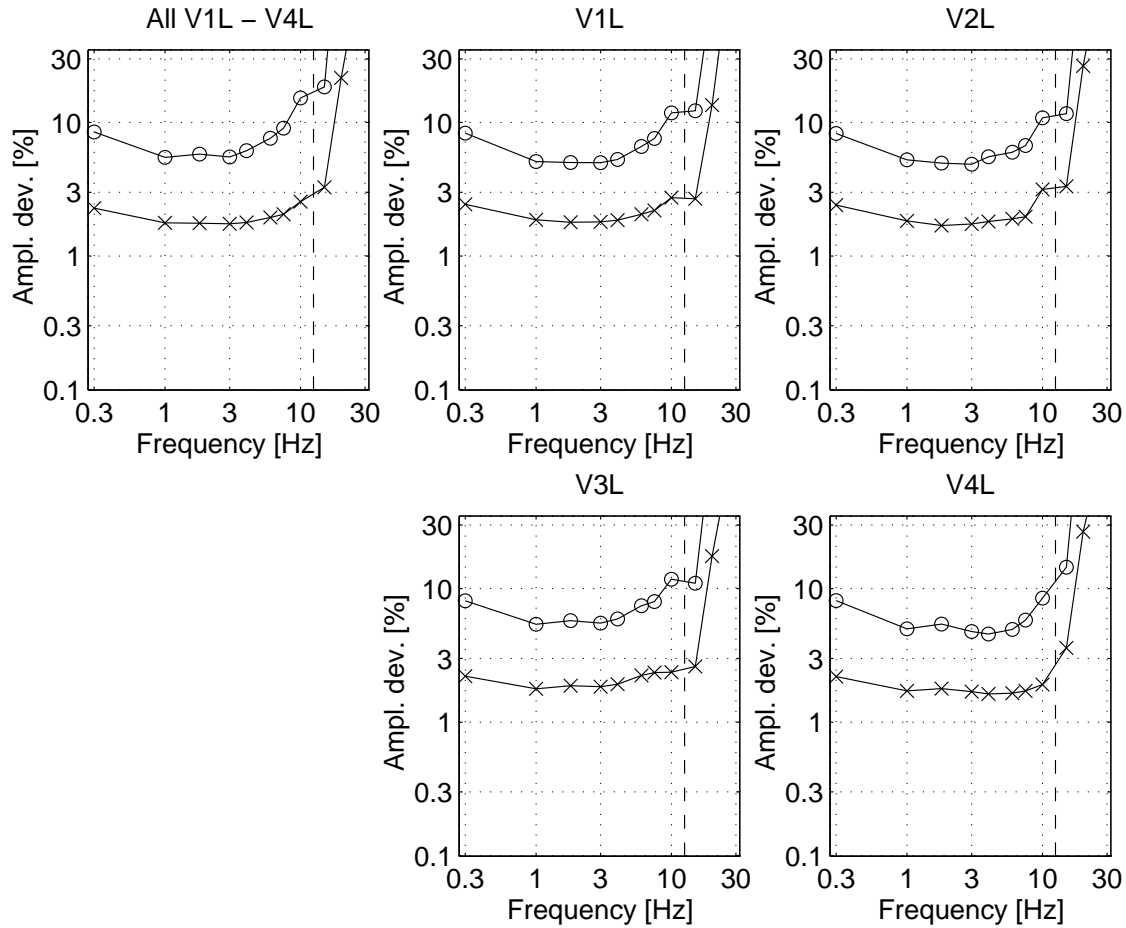


Figure 5: Maximum (circles) and standard (crosses) amplitude deviations between channels for the different EFW models. Nyquist frequency indicated by the dashed line.

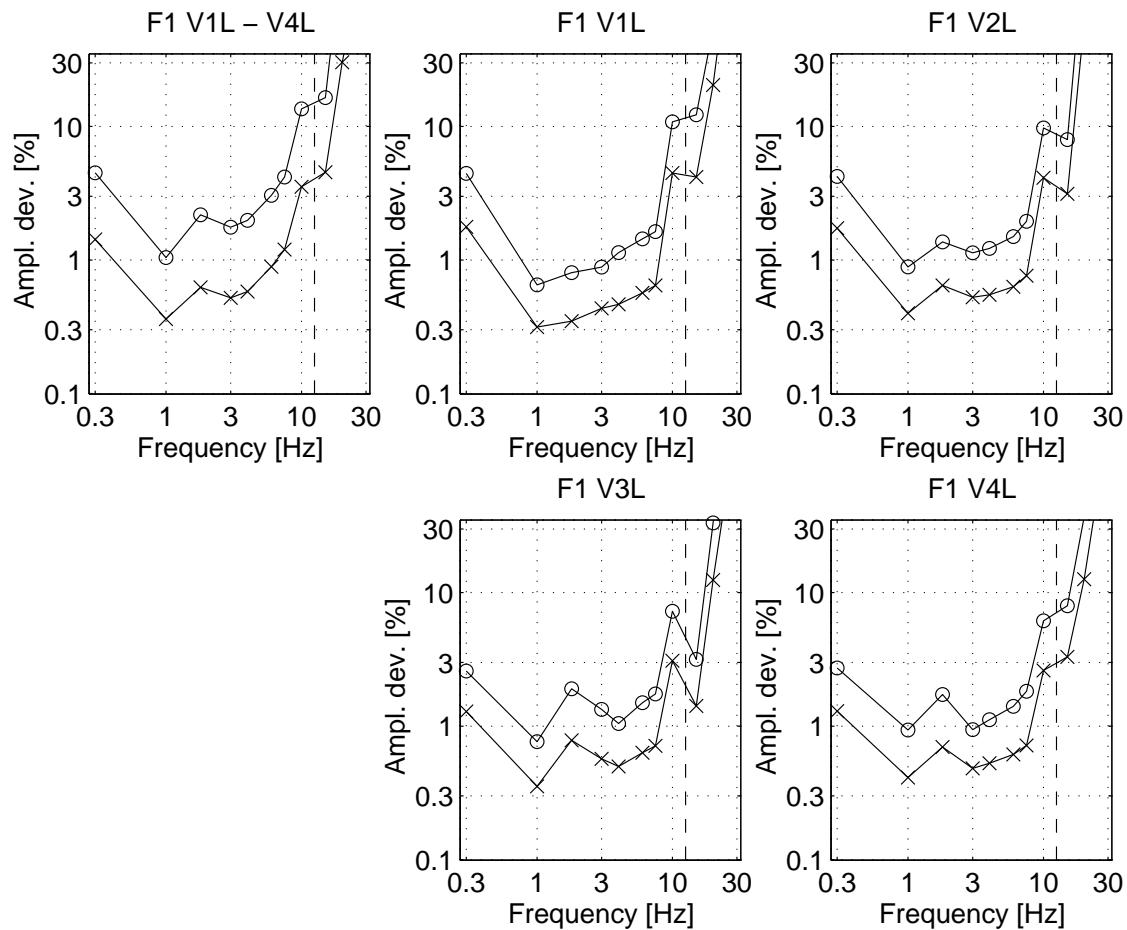


Figure 6: Maximum (circles) and standard (crosses) amplitude deviations for the EFW model F1. Nyquist frequency indicated by the dashed line.

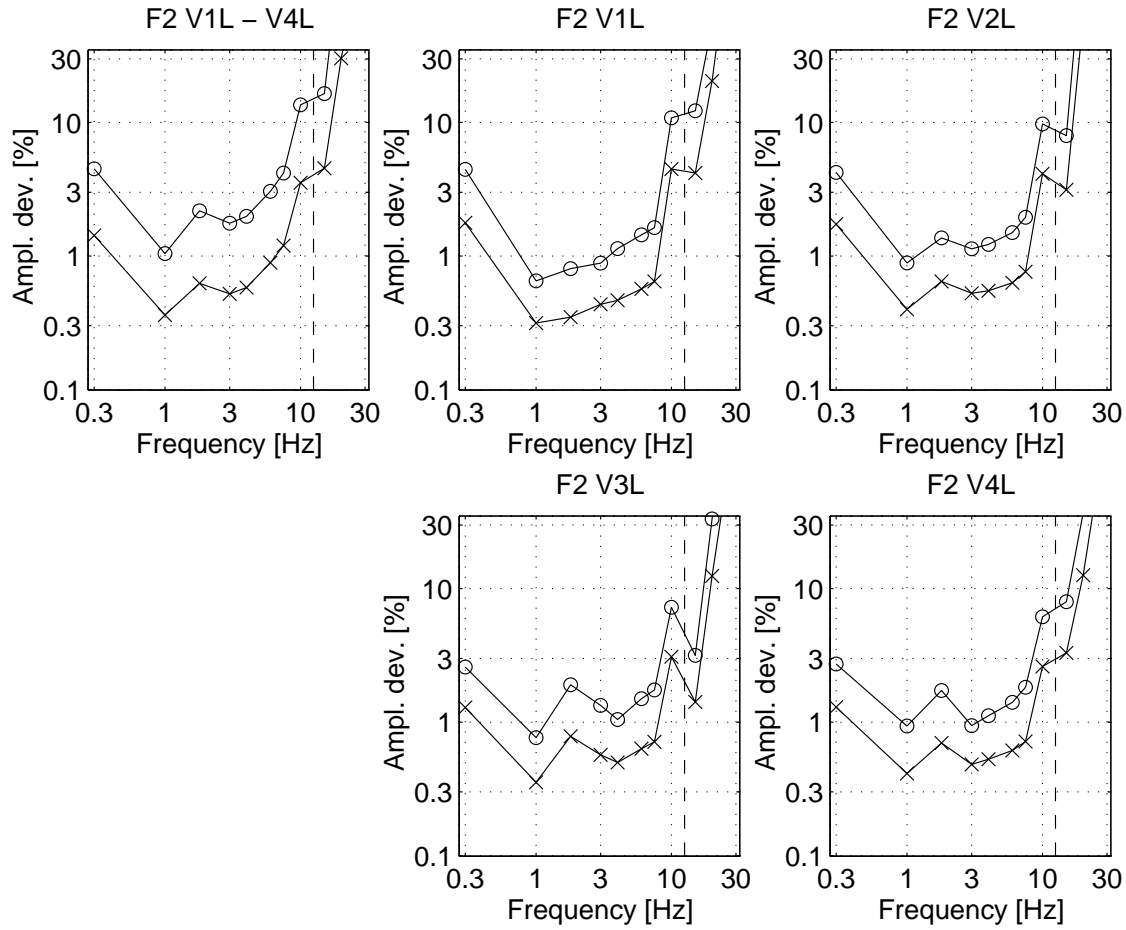


Figure 7: Maximum (circles) and standard (crosses) amplitude deviations for the EFW model F2. Nyquist frequency indicated by the dashed line.

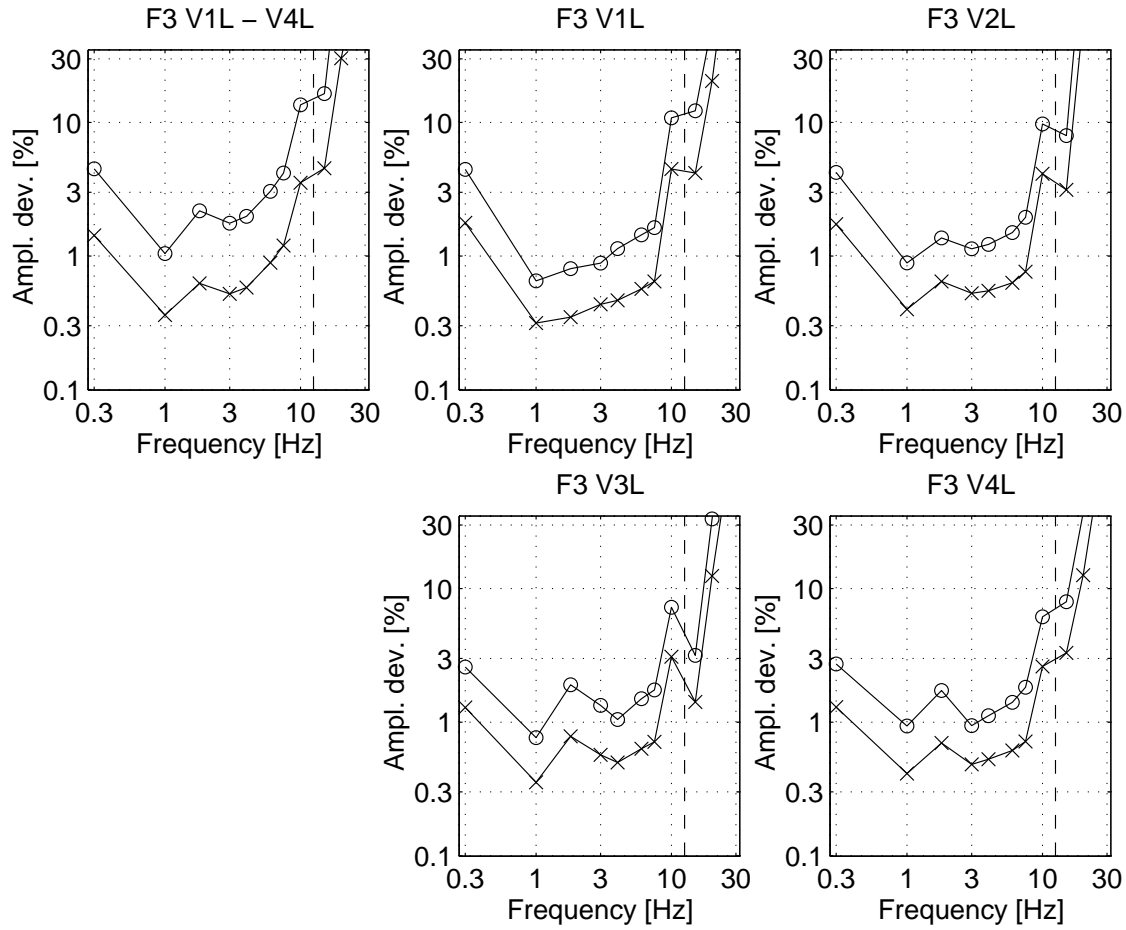


Figure 8: Maximum (circles) and standard (crosses) amplitude deviations for the EFW model F3. Nyquist frequency indicated by the dashed line.

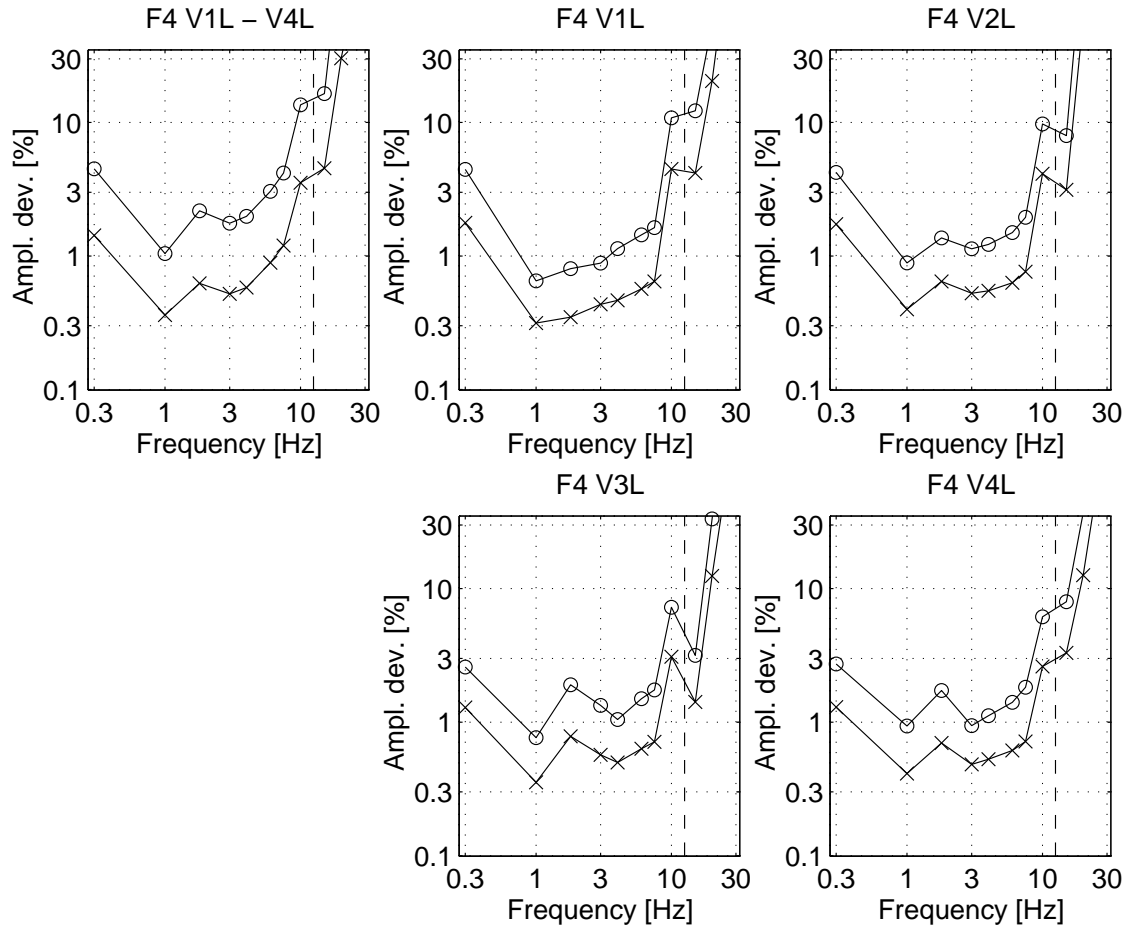


Figure 9: Maximum (circles) and standard (crosses) amplitude deviations for the EFW model F4. Nyquist frequency indicated by the dashed line.

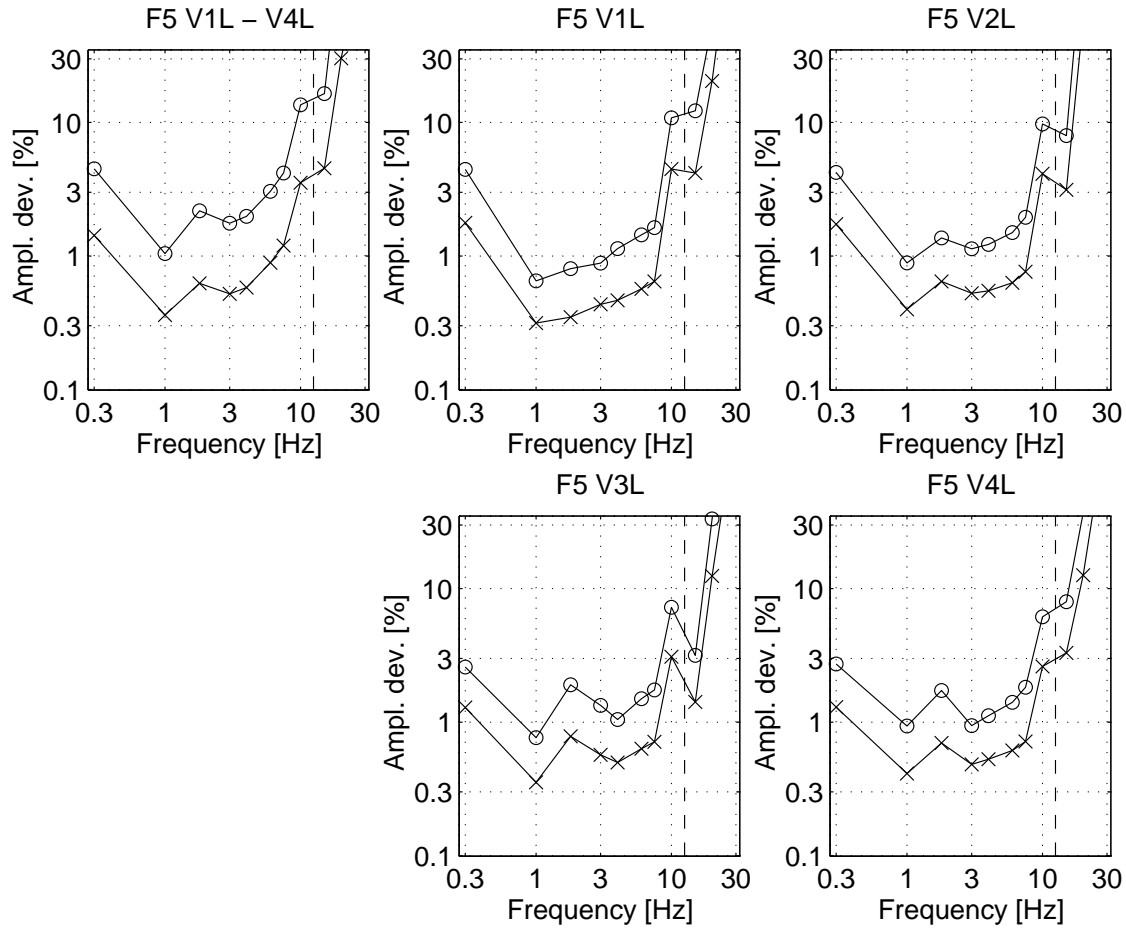


Figure 10: Maximum (circles) and standard (crosses) amplitude deviations for the EFW model F5. Nyquist frequency indicated by the dashed line.

2.9 Reference Documents

- [1] G. Holmgren A. Eriksson and A. Lundgren. Cluster EFW application of calibrations. Technical Report EFW-IRFU-TN-0004, Swedish Institute of Space Physics, Uppsala Division, January 2000.
- [2] L. Åhlén and A. I. Eriksson. Cluster EFW analog calibrations. Technical Report EFW-IRFU-TN-0001, Swedish Institute of Space Physics, Uppsala Division, February 2000.
- [3] G. Gustafsson. A proposal for a spherical double probe electric field experiment for the Cluster mission. Technical report, IRF-U, 1987.
- [4] G Gustafsson, R Boström, B Holback, G Holmgren, A Lundgren, K Stasiewicz, L Åhlén, F S Mozer, D Pankow, P Harvey, P Berg, R Ulrich, A Pedersen, R Schmidt, A Butler, A W C Fransen, D Klinge, M Thomsen, C-G Fälthammar, P-A Lindqvist, S Christenson, J Holtet, B Lybekk, T A Sten, P Tanskanen, K Lappalainen, and J Wygant. The electric field and wave experiment for the Cluster mission. *Space. Sci. Rev.*, 79:137–156, 1997.
- [5] B. Lybekk and M. Thomsen. Content of cluster efw digital calibration directory. Technical Report EFW-UIO-TN-0202, Institute of Physics, University of Oslo, February 1996.
- [6] B. Lybekk and M. Thomsen. Digital calibration of cluster EFW. Technical Report EFW-UIO-TN-0202, Institute of Physics, University of Oslo, February 2000. Replaces EFW-IRFU-TN-0003.
- [7] B. Lybekk and M. Thomsen. Digital calibration of cluster EFW. Technical Report EFW-UIO-TN-0202, Institute of Physics, University of Oslo, February 2000. Replaces EFW-IRFU-TN-0003.